Journal of Modern Optics

ISSN: 0950-0340 (Print) 1362-3044 (Online) Journal homepage: https://www.tandfonline.com/loi/tmop20

Computational terahertz imaging with dispersive objects

M. S. Kulya, N. S. Balbekin, I. V. Gredyuhina, M. V. Uspenskaya, A. P. Nechiporenko & N. V. Petrov

To cite this article: M. S. Kulya, N. S. Balbekin, I. V. Gredyuhina, M. V. Uspenskaya, A. P. Nechiporenko & N. V. Petrov (2017) Computational terahertz imaging with dispersive objects, Journal of Modern Optics, 64:13, 1283-1288, DOI: 10.1080/09500340.2017.1285064

To link to this article: https://doi.org/10.1080/09500340.2017.1285064

JOURNAL OF MODERN OPTICS, 2017
VOL. 64, NO. 13, 1283–1288
https://doi.org/10.1080/09500340.2017.1285064

Taylor & Francis
Taylor & Francis Group

Computational terahertz imaging with dispersive objects

M. S. Kulya, N. S. Balbekin, I. V. Gredyuhina, M. V. Uspenskaya, A. P. Nechiporenko and N. V. Petrov

Department of Photonics and Optical Information Technologies, ITMO University, St. Petersburg, Russian Federation

ABSTRACT

We present measurements of optical characteristics of sodium polyacrylate in the terahertz frequency range and discuss how material dispersion affects object visualisation in terahertz imaging. We demonstrate how important is to take into account the material dispersion for phase and relief reconstruction of the investigated object.

ARTICLE HISTORY
Received 26 July 2016
Accepted 10 January 2017

KEYWORDS
Pulsed terahertz radiation; phase imaging; terahertz pulse time-domain holography; digital holography

1. Introduction

Detection of hidden dielectric objects inside different opaque materials is one of crucial tasks of the modern technology. One of the possible solutions is to use terahertz (THz) imaging since the majority of dielectric media are transparent to the wavelengths of terahertz light. THz radiation also possesses a unique combination of desirable features for imaging. This includes suitable penetration depth; radiation wavelengths in the range of 30–3000 mm, which are diffracted by much bigger objects than visible light; submillimeter resolution in the range from 0.3–10 THz and the ability to obtain spectroscopic information for samples whose spectral features lie in that range. These objects include a variety of explosives, complex organic molecules and polymers. Furthermore, THz radiation is noninvasive due to the low photon energy and may be applied in medicine in biology. Using only the direct detection of the time-domain dependence of THz radiation one can obtain complex spectra and register the information of amplitude and phase of transmitted or reflected wavefronts.

Imaging, visualization of the internal structure of objects, non-destructive testing and holography in the THz frequency range are of considerable interest both for research and for practical applications (*1*–*6*). Currently, a lot of studies in THz imaging are focused on the problem of phase characteristics reconstruction which allows to obtain object's parameters such as complex spatial and/or frequency distribution of the refractive index. Using this distribution, one can obtain entire three-dimensional image of the investigated object (*7*–*10*), as well as provide identification of hidden objects in dispersive materials.

THz imaging is now quickly developing technique becoming more and more actual (*11*–*15*). In (*16*), we describe THz pulse time-domain holography (PTDH) as the ultimate imaging method of amplitude and phase objects reconstruction that provides high resolution in all directions among far-field imaging techniques. In the latter work, we showed the reconstruction of phase object relief using THz PTDH method. In this paper, we consider a new feature of influence of object's dispersion properties on accuracy of relief reconstruction.

Objects which are transparent to the THz light often do not introduce amplitude changes in wavefront sufficient enough for object characterization. However, the information about object relief is encoded in a spatial phase distribution which refers to the refractive index at each frequency component of the incident light. Therefore, by having both amplitude and phase information one can correctly reconstruct the relief of transparent object.

In this paper, we investigate the THz PTDH method and its application for imaging of hidden objects concerning materials with a complex spatial distribution of the optical properties. In contrary to (*16*), present research will further extend the class of objects for which one can apply THz holography method. Polymers are an example of such complex objects. For the correct image reconstruction of the object by the multiwavelength THz PTDH method it is necessary to take into account the phase of each spectral component. Its definition depends on the accuracy of the refractive index measurement.

In our experiment, we used sodium polyacrylate (PA) as a material with significant dispersion variation. Also

CONTACT M. S. Kulya mskulya@corp.ifmo.ru

this material is used in many applications such as medicine, pharmacology, food, mining, oil and gas industry, agriculture and in solving water and environmental problems due to its extra absorptivity. PA is also successfully used in medical and dental practices and manufacture of dentures and teeth, contact lenses, special castings for preservation of various products, bioactive sorbing wound coverings (*17*–*19*). Due to the high water solubility and degree of swelling, such PAs are excellent thickeners and gelling agents, that is why they are widely used in lotions and creams, sunscreen agents. In this case, it remains important to monitor the material properties at different steps of the synthesis of PA and during the development a new generation of materials for various purposes and with wide spectrum of action (*20*).

2. Measurements

2.1. Sample preparation and experiment

Polymer samples were made with a fixed extent of neutralization of acrylic acid (AA) by solution of sodium hydroxide (70%) and with a fixed value of the redox system (tetramethylethylenediamine and ammonium persulphate) and methylenebisacrylamide as a crosslinking agent.

To calculate the dispersion of the test object we performed the series of experiments using the THz time-domain spectrometer (THz TDS) in the transmission mode (*21*, *22*). The scheme of the versatile THz spectrometer is shown in the Figure 1. Photoconductive antenna (undoped InAs) (*23*, *24*) was placed in a constant magnetic field of 2.4 T (*25*). Antenna was illuminated by radiation of femtosecond laser FL -1 (the active medium - Yb: KYW; λ = 1040 nm, t_p = 46 fs, ν = 70 MHz, P = 1,2 W). It allowed obtaining THz radiation of conical form with the following parameters: spectral range from 0.1–2.0 THz, average power 1 μW, pulse duration 2.7 ps. The uppermost radiation energy was obtained in the range of 0.12-1.10 THz.

THz radiation from the source passed through a Teflon filter to cut off the wavelengths which are less than 50 micrometers. Then the radiation was collimated by first parabolic mirror and focused by the second parabolic mirror to the sample with a certain amplitude and phase transmission. The sample was fixed normally to the optical axis in the focal plane using two-axis motorized translation stage. Electro-optical detection was carried out using quarter-wave plate, Wollaston prism, balanced photodetector and lock-in amplifier (*5*, *6*). Filtered and amplified signal was transmitted to a computer via the digitiser. Operation of the setup was realized using NI LabVIEW software. Spectral resolution of the THz spectra was about 7 GHz (*26*).

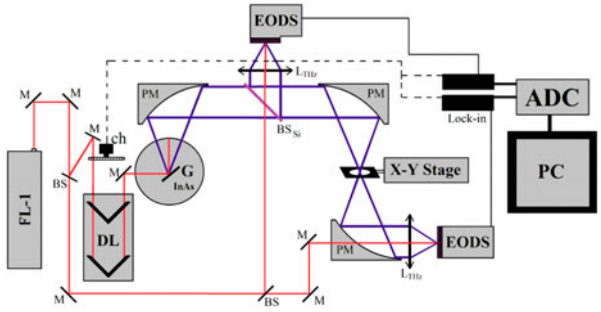

Figure 1. The scheme of versatile THz spectrometer (*22*). FL-1 - femtosecond laser; M - mirrors; BS - beam-splitter; DL - optical delay line; G - THz radiation generator based on InAs; PM - parabolic mirrors; ch - chopper; EODS - electro-optical detection system; lock-in - lock-in amplifier; ADC - analog/digital converter; PC - personal computer.

2.2. Calculation of dispersion characteristics

To determine the optical properties of the sodium PA sample in the terahertz frequency range, we calculated the refractive index of the investigated object and the reference spectrum of terahertz pulse (see Figure 2(a)) (*5*). One can notice the oscillations in the THz pulse tail caused by scheme geometry and water vapor presence in the laboratory air. We used Fast Fourier Transform algorithm (FFT) to calculate the phase of each monochromatic component of the pulse spectrum from the initial distribution of the electric field amplitude of terahertz pulse. Analyzing the difference of spectral phases of the object and reference pulses, we calculated the frequency dependence of the material refractive index using Equation (1a).

$$n(\nu) = 1 + \frac{\Delta\varphi(\nu)c}{2\pi\nu\Delta l}, \tag{1a}$$

where

$$\Delta\varphi(\nu) = \varphi_{obj}(\nu) - \varphi_{ref}(\nu) = \arg\left(FFT\left(E_{obj}\left(t\right)\right)\right) - \arg\left(FFT\left(E_{ref}\left(t\right)\right)\right) \tag{1b}$$

Here c is a speed of light, ν is frequency, Δl is the thickness of the 'S10N4' polymer sample, FFT is fast Fourier transform, E_{ref} is the time-dependent electric field of the reference THz pulse E_{obj} is the time-dependent electric field of the object THz pulse. *Arg* defines angle ϕ of complex number, obtained after Fourier transform from E(t). Physically it defines phase of each monochromatic components.

Dispersion of the refractive index in the range of 0.15–1.5 THz was around 0.6. (See Figure 2(b)).

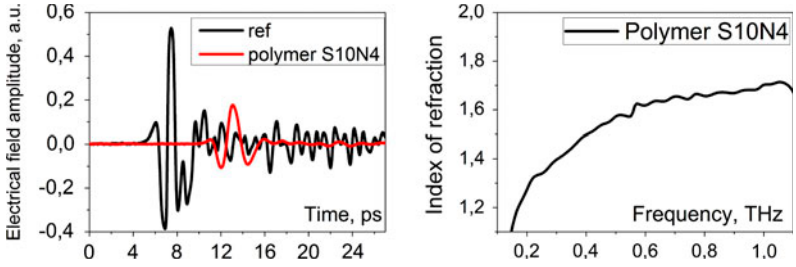

(a) Time dependence of the THz electric field amplitude: black line indicates reference pulse and red line indicates pulse passed through the object.

(b) Dispersion of Sodium PA refractive index obtained from the experimental data.

Figure 2. Refractive index measurement.

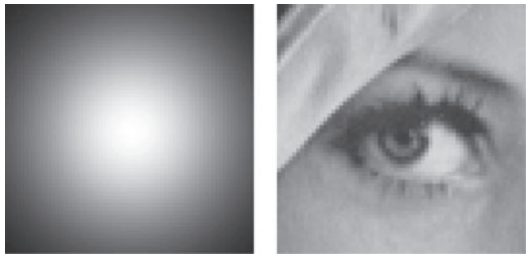

(a) Gaussian amplitude distribution.

(b) Phase distribution.

Figure 3. Initial amplitude (a) and phase (b) distributions of the test object. Object size is 64×64 pixels. Pixel size is 1 mm, the maximum value of the object's height is equal to 1.5 mm.

3. Simulation of dispersive object reconstruction

The resulting frequency dependence of the refractive index was used to extract the initial phase of individual frequency components of the test object Fourier spectrum. As the amplitude mask of the test object, we used a Gaussian distribution (Figure 3(a)) and as a phase mask we used the image with a gradient relief 'Lena's eye' (Figure 3(b)). Modeling of hologram recording and reconstruction was carried out using THz PTDH method. The wavefront propagation was calculated numerically based on the method of the field representation through the angular spectrum (AS) of plane waves and Rayleigh–Sommerfeld convolution method (RSC). More detailed information about terahertz pulse time-domain holography method can be found in (*16*).

The calculation of hologram recording and reconstruction was performed for the cases with $n = n(\nu)$ and $n = const$. After that, we obtained spatial frequency distribution of the phase in the object plane. Figure 4 shows the phase portraits of reconstructed holograms at different frequencies of THz spectrum for the case with dispersion (Figure 4(a)) and without dispersion (Figure 4(b)) of the refractive index. When comparing the images obtained at the same frequencies, the differences in the phase shift are clearly observed. This difference is caused by the additional phase shift in the case with dispersion when $n = n(\nu)$.

Figure 4(c) shows a cross section of the phase surfaces for images at frequencies of 0.2, 0.3, 0.4 and 0.5 THz for the cases with and without dispersion. From the graphs in the Figure 5 we can see irregular phase delay behavior, which is obtained by comparing the phase increment at a single image point. These curves show the different dynamics of the phase shift. It is obvious that dispersion accounting causes a change in the phase retard in the frequency domain. It should be noted that the nature of the phase retardation is similar to the dispersion curve in Figure 2(b). Phase distribution at single point allows obtaining relief distribution (Figure 5(b)):

$$h(x_0, y_0) = \frac{\Delta\varphi(x_0, y_0)c}{2\pi\nu_i(n(\nu_i) - 1)}. \tag{2}$$

For the transition from the phase characteristics at all frequencies to the profile of the object, it is necessary to take into account the dispersion of the material and reconstruct the total image using all frequencies. Mathematically, the relief structure calculation in the case when the object consists of a homogeneous material will have the form:

$$h(x_0, y_0) = \frac{\sum_{i=1}^{m} \frac{\Delta\varphi(x_0,y_0)c}{2\pi\nu_i(n(\nu_i)-1)}}{m}. \tag{3}$$

Here, x_0 and y_0 are coordinates in the object plane, ν_i values of each frequency in the THz spectrum, m is the number of frequencies in spectrum.

Thus, if we use for the dispersive media $n(\nu)$ = constant instead of $n(\nu)$ during relief reconstruction we obtain incorrect profile-frequency dependence, which leads to inaccuracy after multi-wavelength composition.

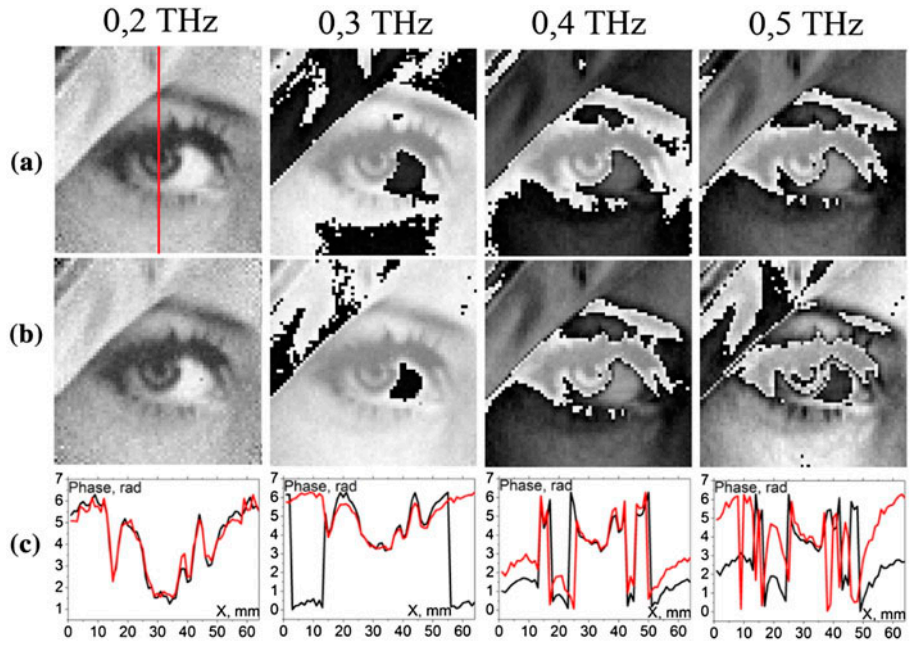

Figure 4. (a) Reconstructed phase images without considering dispersion. (b) Reconstructed phase images with considering dispersion at different frequencies in THz range. (c) Images cross sections: black line is for case (a), red line is for case (b).

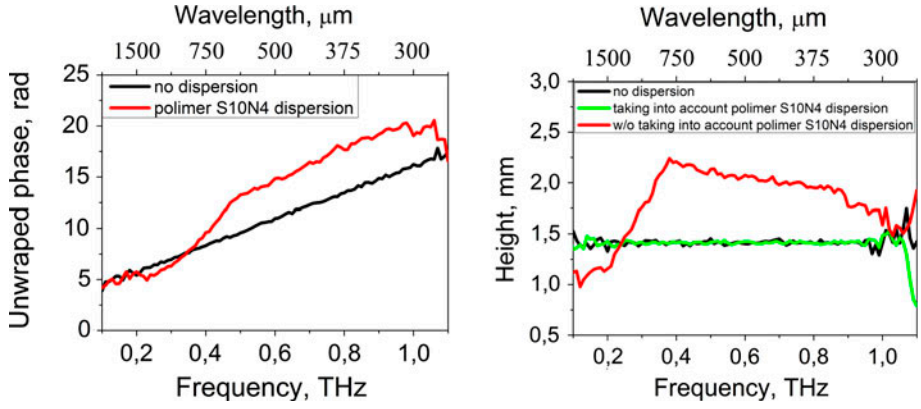

(a) Changes in phase retardation observed at the image point (x = 5, y = 35).

(b) Dependence of the object height in frequency domain at the image point (x = 5, y = 35)

Figure 5. Characteristics of the reconstructed object at a single point.

In the case of an inhomogeneous object, we have to take all the spectral components in each point of the object plane and consider their impact on the relief pattern reconstruction. However, the impact of the individual frequency components will be ambiguous, as if we disregard the phase shift due to material dispersion. Therefore, the dispersion of material in object relief reconstruction is essential. This fact is illustrated in Figure 6, which shows total reconstructed object relief without considering dispersion, considering dispersion and in the case of taking into account dispersion while hologram recording, but excluding dispersion during the hologram reconstruction. If we do not take into account the dispersion during transition from phase to relief with the equation (4), it will change the reconstructed phase relief, which is critical for investigation of the object hidden in a dispersive medium.

This fact is shown in Figure 6, which illustrates the surface cross section of the reconstructed object for the cases when the refractive index is assumed to be constant during the calculation (Figure 6, black line), when the refractive index is a frequency-dependent function (Figure 6, green line) and in the case when frequency dependence of the refractive index is taken into account only when the hologram is recorded, but missed during relief reconstruction (Figure 6, red line).

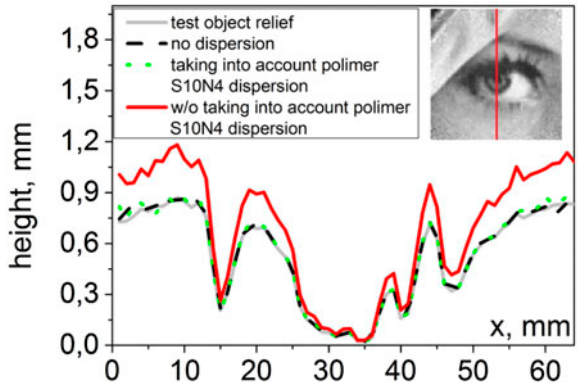

Figure 6. Cross sections of the reconstructed object (inset in the upper-right corner): grey line shows initial test-object relief. Black line indicates the reconstructed total multi-wavelength relief simulated without dispersion, green line shows the object relief reconstructed considering the dispersion, red line shows the object relief reconstructed considering dispersion during the hologram recording, but excluding dispersion during relief reconstruction.

4. Summary

In this study, we showed the importance of taking into account the dispersion of the test object in the case of THz imaging, holography and tomography, where the accuracy of phase characteristics determination is directly related to taking into account the refractive index of the materials. We have shown how the dispersion of the refractive index of the material affects the accuracy of phase characteristics of diffracted field in the terahertz multi-wavelength holographic approach (THz PTDH) to the problem of visualization and test object relief reconstruction. Phase uncertainty problem arising as a result of not considering the dispersion is especially significant in the case of image reconstruction of an object with complex spatial-frequency distribution of the refractive index. In comparison with (*14*) we expanded a class of objects for holographic relief reconstruction, expanding it for dispersive materials. The above features will have extra significance in solving problems of finding objects hidden in a complex all dispersive medium.

Disclosure statement

No potential conflict of interest was reported by the authors.

Funding

The work of N.V. Petrov and N.S. Balbekin was supported by the Russian Ministry of Education and Science project within the state mission for institutions of higher education [Agreement 2014/190]. M.S. Kulya acknowledges the financial support from the Ministry of Education and Science of the Russian Federation [grant number 3.1675.2014/K].

ORCID

M. S. Kulya http://orcid.org/0000-0001-5056-4793

References

(1) Tonouchi, M. Cutting-Edge Terahertz Technology. *Nat. Photonics.* **2007,** *1,* 97–105.
(2) Kleine-Ostmann, T.; Nagatsuma, T. A Review on Terahertz Communications Research. *J. Infrared Millim. Te.* **2011,** *32,* 143–171.
(3) Song, H.-J.; Nagatsuma, T. Present and Future of Terahertz Communications. *IEEE Trans. Terahertz Sci. Technol.* **2011,** *1,* 256–263.
(4) Xue, K.; Li, Q.; Li, Y.-D.; Wang, Q. Continuous-Wave Terahertz In-Line Digital Holography. *Opt. Lett.* **2011,** *36,* 1993–1995.
(5) Zhang, X.C. In *Introduction to THz Wave Photonics*, Zhang, X.C., Xu, J., Eds.; Springer: New York, 2010. Vol. 29, 246.
(6) Lee, Y.-S. In *Principles of Terahertz Science and Technology*, Lee, Y.-S., Eds.; Springer Science & Business Media: 2009. Vol. 170, 340.
(7) Hu, B.B.; Nuss, M.C. Imaging with Terahertz Waves. *Opt. Lett.* **1995,** *20,* 1716–1718.
(8) Mittleman, D.; Jacobsen, R.; Nuss, M.C. T-Ray Imaging. *Quantum Electron+.* **1996,** *2,* 679–692.
(9) Mittleman, D.; Gupta, M.; Neelamani, R.; Baraniuk, R.; Rudd, J.; Koch, M. Recent Advances in Terahertz Imaging. *Appl. Phys.* **1999,** *68,* 1085–1094.
(10) Wang, S.; Ferguson, B.; Abbott, D.; Zhang, X.-C. T-ray Imaging and Tomography. *J. Biol. Phys.* **2003,** *29,* 247–256.
(11) Heimbeck, M.S.; Kim, M.K.; Gregory, D.A.; Everitt, H.O. Terahertz Digital Holography using Angular Spectrum and Dual Wavelength Reconstruction Methods. *Opt. Exp.* **2011,** *19,* 9192–9200.
(12) Knyazev, B.A.; Cherkassky, V.S.; Choporova, Y.Y.; Gerasimov, V.V.; Vlasenko, M.G.; Demyanenko, M.A.; Esaev, D.G. Real-Time Imaging Using a High-Power Monochromatic Terahertz Source: Comparative Description of Imaging Techniques with Examples of Application. *J. Infrared Millim. THz Waves.* **2011,** *32,* 1207–1222.
(13) Choporova, Y.Y.; Knyazev, B.A.; Mitkov, M.S. Classical Holography in the Terahertz Range: Recording and Reconstruction Techniques. *IEEE Trans. Terahertz Sci. Technol.* **2015,** *5,* 836–844.
(14) Ahi, K.; Anwar, M. In *Developing Terahertz Imaging Equation and Enhancement of the Resolution of Terahertz Images using Deconvolution*, SPIE Commercial+ Scientific Sensing and Imaging, International Society for Optics and Photonics, 2016. pp. 98560N–98560N-18.
(15) Ahi, K.; Anwar, M. In *Modeling of Terahertz Images Based on X-ray Images: A Novel Approach for Verification of Terahertz Images and Identification of Objects with Fine Details Beyond Terahertz Resolution*, SPIE Commercial+ Scientific Sensing and Imaging, International Society for Optics and Photonics, 2016. pp. 985610–985610-9.
(16) Petrov, N.V.; Kulya, M.S.; Tsypkin, A.N.; Bespalov, V.G.; Gorodetsky, A.A. Application of Terahertz Pulse Time-Domain Holography for Phase Imaging. *IEEE Trans. Terahertz Sci. Technol.* **2016,** *6,* 464–472.

(17) Kamyo, Y.; Fujimoto, H.; Kawaguchi, H.; Yuguchi, Y.; Urakawa, H.; Kajiwara, K. Preparation and Structural Characterization of Hydrogen Microsheres. *Polym. J.* **1996,** *28,* 309–316.
(18) Shvareva, G.N.; Ryabova, Ye.N.; Shatskiy, O.V. Superabsorbents Based on Acrylates (Methacrylates) and Aspects their Usage. *J. Plasticheskie Massy* **1996,** *3,* 32-35.
(19) Smirnov, S.V.; Grachev, Ya.V.; Tsypkin, A.N.; Bespalov, V.G. Experimental Studies of the Possibilities of Diagnosing Caries in the Solid Tissues of a Tooth by Means of Terahertz Radiation. *J. Opt. Tech.* **2014,** *81,* 464-467.
(20) Krumbholz, N.; Hochrein, T.; Vieweg, N.; Hasek, T.; Kretschmer, K.; Bastian, M.; Koch, M. Monitoring Polymeric Compounding Processes Inline with THz Time-Domain Spectroscopy. *Polym. Test.* **2009,** *28,* 30–35.
(21) Bespalov, V.G.; Gorodetski, A.A.; Denisyuk, I.Yu.; Kozlov, S.A.; Krylov, V.N.; Lukomski, G.V.; Petrov, N.V.; Putilin, S.E. Methods of Generating Superbroadband Terahertz Pulses with Femtosecond Lasers. *J. Opt. Technol.* **2008,** *75,* 636–642.
(22) Balbekin, N.S.; Grachev, Y.V.; Smirnov, S.V.; Bespalov, V.G. The Versatile Terahertz Reflection and Transmission Spectrometer with the Location of Objects of Researches in the Horizontal Plane. *J. Phys. Conf. Ser.* **2015,** *584,* 012010.
(23) Gärtler, A.; Winnewisser, C.; Helm, H.; Jepsen, P. Terahertz Pulse Propagation in the Near Field and the Far Field. *J. Opt. Soc. Am. A* **2000,** *17,* 74–83.
(24) Izumida, S.; Ono, S.; Liu, Z.; Ohtake, H.; Sarukura, N. Spectrum Control of THz Radiation from InAs in a Magnetic Field by Duration and Frequency Chirp of the Excitation Pulses. *Appl. Phys. Lett.* **1999,** *75,* 451–453.
(25) Mittleman, D.M.; Cunningham, J.; Nuss, M.C.; Geva, M. Noncontact Semiconductor Wafer Characterization with the Terahertz Hall Effect. *Appl. Phys. Lett.* **1997,** *71,* 16–18.
(26) Chan, W.L.; Deibel, J.; Mittleman, D.M. Imaging with Terahertz Radiation. *Rep. Prog. Phys.* **2007,** *70,* 1325.